173.7-Tb/s Triple-Band WDM Transmission using 124-Channel 144-GBaud Signals with SE of 9.33 b/s/Hz

Fukutaro Hamaoka, Masanori Nakamura, Minami Takahashi, Takayuki Kobayashi, Yutaka Miyamoto, and Yoshiaki Kisaka
NTT Network Innovation Laboratories, NTT Corporation, 1-1 Hikari-no-oka, Yokosuka, Kanagawa, 239–0847 Japan
fukutaro.hamaoka.xz@hco.ntt.co.jp

Abstract: We demonstrate 173.7-Tb/s 101-km transmission in an 18.6-THz bandwidth, achieving a 9.33-b/s/Hz spectral efficiency at 144 GBaud with 124-WDM channels of net bitrates between 1.18 and 1.54 Tb/s/wavelength using entropy and code-rate optimized PCS-64QAM signals.

1. Introduction

Large-capacity and cost-effective optical transport systems with high-speed digital coherent transceivers are necessary to cope with the rapid increase in communication traffic. In such scenarios, the per-wavelength transceiver capacity (b/s/λ) must be enlarged to accommodate high-speed client signals, i.e., the next-generation Ethernet [1]. >1-Tb/s/λ digital-coherent transmission technologies have been intensively studied with high-symbol-rate 100- to 200-GBaud signals, and we reached the multi-Terabit (>2-Tb/s/λ) capacity recently [2]. Furthermore, wavelength division multiplexed (WDM) transmission using >1-Tb/s signals with a high-symbol rate is suitable for long-haul transmission [3, 4] and reducing system complexity, i.e., decreasing the required number of transceivers to fill an optical band [3, 5, 6]. To increase the system capacity to >100 Tb/s, using multiple-band WDM transmission technologies is essential while enhancing the spectral efficiency (SE) with high-order quadrature amplitude modulation (QAM) signals. Dual-band (C and L or extended L bands) [7–9] and triple-band WDM transmission with an additional S band [10–17] using single-mode fiber (SFM) have been reported with capacities of greater than 100 to 200 Tb/s. Focusing on the per wavelength average net bitrate and WDM grid shown in Fig. 1 in wideband (double and triple-band) WDM experiments involving >100-Tb/s SMF transmission, these are respectively limited to up to 0.853 Tb/s/λ and up to 75 GHz because the symbol rate was restricted to 70 GBaud to achieve a high SE of >11 b/s/Hz [17].

In this paper, we applied a high-symbol-rate transmission technology [2] to a triple-band (S, C, and extended L bands) WDM system. The entropy and code-rate optimization scheme [2, 18] enabled the per wavelength net bitrates of WDM channels to be between 1.18 and 1.54 Tb/s/λ (an average net bitrate of 1.4 Tb/s/λ) using 144-GBaud probabilistically constellation-shaped (PCS) 64QAM. A 173.7-Tb/s capacity over 101-km SMF transmission was achieved by using 124-channel signals within a 150-GHz WDM grid under an 18.6-THz triple-band WDM configuration. As can be seen in Fig. 1(a), to the best of our knowledge, this is the first demonstration of a >100-Tb/s capacity with the highest per wavelength average net bitrate among wideband WDM transmission experiments. As shown in Fig. 1(b), a high SE of 9.33 b/s/Hz at 144 GBaud in a 150-GHz WDM grid was achieved while doubling the symbol rate from the previous reports [16, 17]. This can reduce the system complexity; we achieved triple-band WDM transmission with the smallest number of 124-WDM channels compared with that between 226 and 793 in previous experiments [10-17].

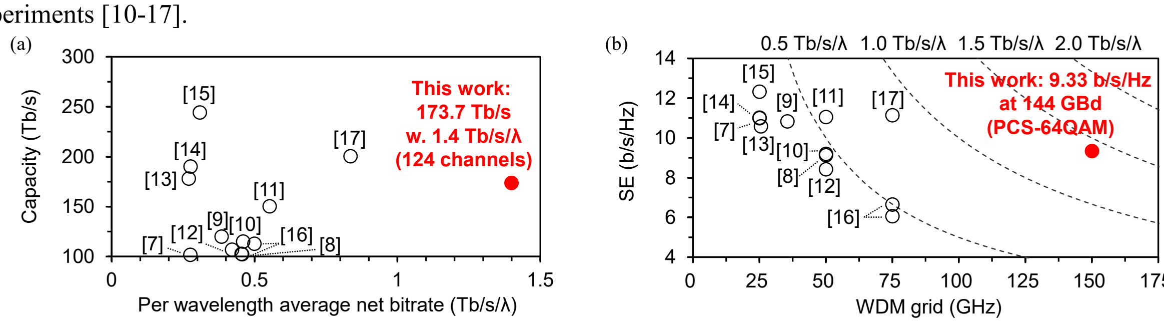

Fig. 1. Trends in >100-Tb/s capacity using wideband WDM technology in SMF transmission experiments: (a) capacity vs. per wavelength average net bitrate and (b) spectral efficiency vs. WDM grid in which contours indicate per wavelength average net bitrate.

2. Experimental Setup

Figure 2(a) shows the experimental setup for triple-band (S, C, and extended L bands) transmission experiments. The high-symbol-rate 144-GBaud signals, which were prepared with offline transmitter-side digital signal processing (Tx-

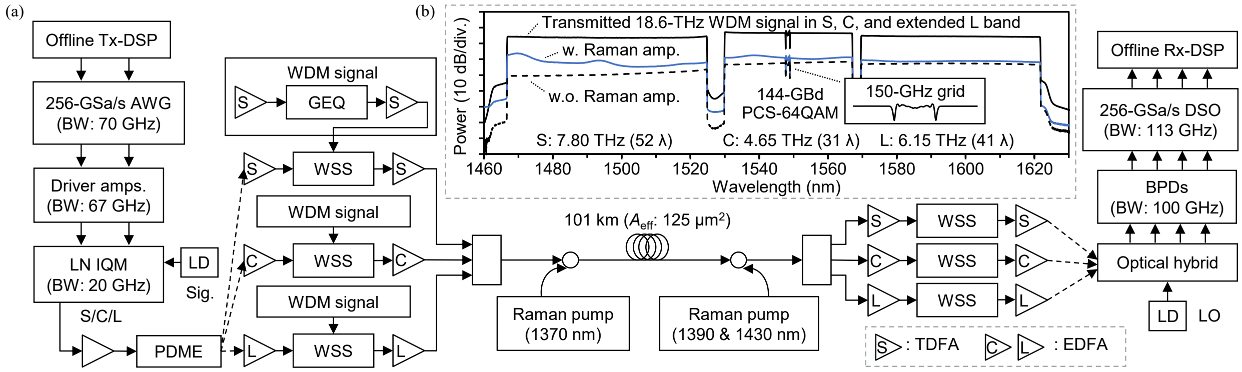

Fig. 2. (a) Experimental setup for S, C, and extended L-band 124-WDM channel transmission with high-symbol-rate 144-GBaud PCS-64QAM signals and (b) optical spectra of transmitted WDM signal and after 101-km transmission with and without Raman amplifiers.

DSP), were generated from a 256-GSa/s arbitrary waveform generator (AWG) having a bandwidth (BW) of 70 GHz. The electrical signals from the AWG through the 67-GHz driver amplifiers were modulated in a lithium niobate IQ modulator (LN-IQM) with a 20-GHz BW. Tx-DSP consists of a third-order Volterra filter to compensate for the nonlinearity of the driver amplifiers [19] and a root-raised-cosine filter with a roll-off factor of 0.3 for up-sampling. After amplifying the modulated signal in a thulium-doped fiber amplifier (TDFA) for the S band and erbium-doped fiber amplifiers (EDFAs) for the C and L band, a polarization division multiplexed (PDM) 144-GBaud PCS-64QAM signal was output from a PDM emulator (PDME) consisting of polarization beam combiners, a delay line, and variable optical attenuators.

The WDM signals in the S, C, and extended L bands were emulated using amplified spontaneous emissions from the optical amplifiers where the optical spectra were flattened using flexible-grid wavelength selective switches (WSS) acting as a gain equalizer (GEQ). The main signal of 144-GBaud PCS-64QAM was multiplexed with the WDM signal in a flexible-grid WSS for each S, C, and extended L band. The frequency response of the main signal was also optically equalized in the WSS. Then, the WDM signals in the S, C, and extended L bands were multiplexed in a WDM coupler as a 150-GHz-grid triple-band WDM signal with a total bandwidth of 18.6 THz as shown in Fig. 2(b). The total fiber input power was 23.49 dBm with 124-WDM channels; the fiber input power in the S, C, and extended L bands were 17.66, 19.15, and 19.21 dBm with 52-, 31-, and 41-WDM channels, respectively. The center wavelength (frequency) ranges of the 150-GHz-grid main signal in this experiment were respectively 1466.695–1524.885 nm (196.60–204.40 THz) in the S band, 1529.994–1567.133 nm (191.30–195.95 THz) in the C band, and 1569.594–1621.815 nm (184.85–191.00 THz) in the extended L band. The transmission line was a 101-km large-core low-loss fiber compliant with ITU-T G.654.E having an effective area (A_{eff}) of 125 μm^2. We used a forward-pumped distributed Raman amplifier at a wavelength of 1370 nm with a power of 421 mW and a backward-pumped distributed Raman amplifier at 1390 nm with 206 mW and at 1430 nm with 93 mW.

The triple-band WDM signal was divided into each S-, C-, and L-band WDM signal after 101-km fiber transmission. A WSS for each band demultiplexed the main signal from the WDM signal, and the main signal was then received using an optical hybrid with an optical local oscillator (LO) and 100-GHz-BW balanced photodetectors (BPDs). The received signal was digitized in a 256-GSa/s digital storage oscilloscope (DSO) with a 113-GHz BW. In an offline receiver-side (Rx) DSP, a frequency domain 8×2 MIMO adaptive equalizer [19] simultaneously compensated for the Tx- and Rx- linear responses of the received signal with a pilot-based digital phase-locked loop using the pilot QPSK symbol every 64 symbol duration. Then, a bit-metric decoder [20] calculated the log-likelihood ratios.

3. Results and Discussion

In the wideband WDM configuration, inter-band stimulated Raman scattering (SRS) occurs among the S, C, and extended L bands. We, therefore, evaluated the effect of the inter-band SRS under the 18.6-THz triple-band WDM configuration. Figure 3(a) shows a link loss, transmission loss under the presence of inter-band SRS, and that with the Raman amplifiers. The link loss included the losses of the 101-km fiber and a WDM coupler used for the backward-distributed Raman amplifier. Figure 3(b) shows the signal power transfer by the inter-band SRS, which was the difference between the link loss and the transmission loss under inter-band SRS from Fig. 3(a). The signal power transition was mainly observed from the S band to the extended L band. In this experiment, we used forward- and backward-pumped distributed Raman amplifiers to compensate for the excess power loss in the S band with the inter-band SRS. As expected, the transmission losses were drastically reduced by the Raman amplifiers (see blue line in Fig. 3(a)) with the sufficient Raman gain shown in Fig. 3(c).

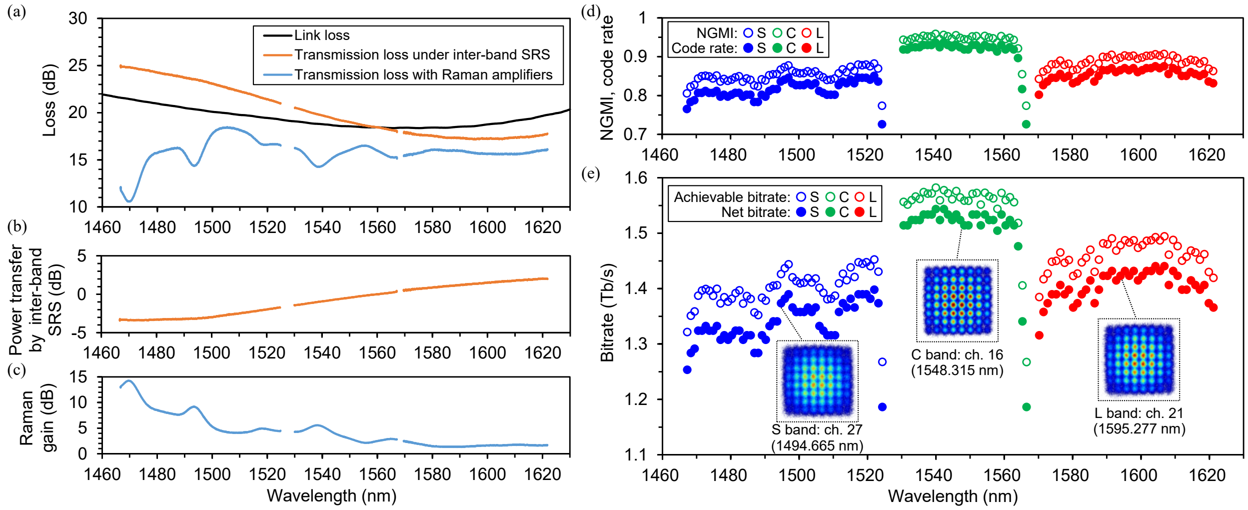

Fig. 3. Experimental results of wavelength dependencies on (a) 101-km link loss, transmission loss under inter-band SRS, and that with Raman amplifier, (b) signal power transition by inter-band SRS after 101-km transmission, (c) Raman on-off gain, (d) NGMI and required code rate, and (e) achievable and net bitrate.

We conducted the 18.6-THz triple-band transmission experiment with 124-WDM channels of the 144-GBaud PCS-64QAM signals. Figure 3(d) shows the wavelength dependencies on the main signal for the normalized generalized mutual information (NGMI) and required code rate of the main signal after 101-km transmission. To enable rate adaptive coding [21], a family of DVBS2 low-density parity-check (LDPC) codes [22] with a puncturing method [23] was used to determine the required code rate for error-free decoding, which assumes outer hard-decision (HD) FEC with a code rate of 0.9922 and BER threshold of 5×10^{-5} [24]. More than 1200 codewords were examined for LDPC decoding. We calculated the wavelength dependencies on the achievable and net bitrate of the main signal from the NGMI and code rate, respectively:

$$C = [2 \cdot \{H_{2D} - (1 - R) \cdot \log_2 M\} \cdot B] \,/\, (1 + P_{OH}/100)\,, \qquad (1)$$

where H_{2D} is the constellation entropy per 2D symbol, R is the NGMI or code rate, M is the modulation order of the QAM, B is the symbol rate, and P_{OH} is the pilot overhead (OH). In this experiment, we used 144-GBaud PCS-64QAM with an entropy of 5.829 bit/2Dsymbol determined by the optimization scheme [18] and with a pilot OH of 1.5873%. The achievable and net bitrate after 101-km transmission for each 124-WDM channel in the S, C, and extended L bands are shown in Fig. 3(e). The total achievable bitrate was 180.6 Tb/s, and the total net bitrate, which means the total capacity of the 101-km transmission results, was 173.7 Tb/s with an SE of 9.33 b/s/Hz using the 124-WDM channels of net bitrates between 1.18 and 1.54 Tb/s/λ (an average net bitrate of 1.4 Tb/s/λ).

4. Conclusion

We demonstrated 18.6-THz triple-band (S, C, and extended L bands) WDM transmission in 150-GHz grids using 144-GBaud PCS-64QAM signals. A capacity of 173.7 Tb/s over 101-km SMF transmission with an SE of 9.33 b/s/Hz was achieved by optimizing the entropy and code rate of 124-WDM channels between 1.18 and 1.54 Tb/s/λ with a rate adaptive coding technique. The experimental demonstration indicates that using >1-Tb/s/λ high-symbol-rate WDM channels can reduce the system complexity for >100-Tb/s-class wideband WDM transmission.

References

[1] Ethernet Alliance, "2022 Ethernet Roadmap," https://ethernetalliance.org/technology/ethernet-roadmap/
[2] M. Nakamura, *et al*., ECOC2022, Th3C.1.
[3] T. Kobayashi, *et al*., OFC2019, Th4B.2.
[4] M. Nakamura, *et al*., OFC2022, W3C.1.
[5] F. Pittalà, *et al*., IEEE Photon. Technol. Lett., 34 (3), 157, (2022).
[6] F. Hamaoka, OFC2020, W3E.1.
[7] D. Qian, *et al*., OFC/NFOEC2011, PDPB5.
[8] A. Sano, *et al*., OFC/NFOEC2012, PDP5C.3.
[9] M. Ionescu, *et al*. ECOC2018, Mo4G.2.
[10] J. Renaudier, *et al*., ECOC2017, Th.PDP.A.3.
[11] F. Hamaoka, *et al*., ECOC2018, Mo4G.1.
[12] J. Renaudier, *et al*., OFC2019, Tu3F.2.
[13] L. Galdino, *et al*., IEEE Photon. Technol. Lett., 32 (17), 1021 (2020)
[14] B. J. Puttnam, *et al*., OFC2021, Th4C.2.
[15] B. J. Puttnam, *et al*., Opt. Express, 30 (6), 10011 (2022).
[16] F. Hamaoka, *et al*., OECC/PSC2022, PDP-A-3.
[17] X. Zhao, *et al*., ECOC2022, Th3C.4.
[18] M. Nakamura, *et al*., ECOC2022, We3C.5.
[19] M. Nakamura, *et al*., OFC2022, M3H.1.
[20] G. Böcherer, et al., IEEE Trans. Commun., 63 (12), 4651 (2015).
[21] A. Ghazisaeidi, *et al*., J. Lightw. Technol., 33 (7), 1479 (2015).
[22] ETSI, EN 302 307-1, v.1.4.1, 2014.
[23] T. Yoshida, *et al*., OFC2018, M4E.5.
[24] D. S. Millar, *et al*., J. Lightw. Technol., 34 (6), 1453 (2016).